Molecular Simulation, 2014
Vol. 00, No. 0, 1–10, http://dx.doi.org/10.1080/08927022.2014.904514

Taylor & Francis
Taylor & Francis Group

Quantum chemical topological analysis of hydrogen bonding in HX···HX and CH_3X···HX dimers (X = Br, Cl, F)

Rodrigo A. Cormanich[a], Regis T. Santiago[b], Felipe A. La Porta[c], Matheus P. Freitas[d], Roberto Rittner[a]*, Elaine F. F. da Cunha[d], Juan Andres[e], Elson Longo[a] and Teodorico C. Ramalho[d]

[a]*Chemistry Institute, State University of Campinas, P.O. Box 6154, 13083-970 Campinas, SP, Brazil;* [b]*Chemistry Institute of São Carlos, University of São Paulo, P.O. Box 780, 13560-970 São Carlos, SP, Brazil;* [c]*Chemistry Institute, Paulista State University, P.O. Box 355, 14801-970 Araraquara, SP, Brazil;* [d]*Department of Chemistry, Federal University of Lavras, P.O. Box 3037, 37200-000 Lavras, MG, Brazil;* [e]*Department of Analytical and Physical Chemistry, Univ. Jaume I, Castelló de la Plana 12071, Spain*

(*Received 10 November 2013; final version received 10 March 2014*)

We present a systematic investigation of the nature and strength of the hydrogen bonding in HX···HX and CH_3X···HX (X = Br, Cl and F) dimers using *ab initio* MP2/aug-cc-pVTZ calculations in the framework of the quantum theory of atoms in molecules (QTAIM) and electron localisation functions (ELFs) methods. The electron density of the complexes has been characterised, and the hydrogen bonding energy, as well as the QTAIM and ELF parameters, is consistent, providing deep insight into the origin of the hydrogen bonding in these complexes. It was found that in both linear and angular HX···HX and CH_3X···HX dimers, F atoms form stronger HB than Br and Cl, but they need short (~2 Å) X···HX contacts.

Keywords: hydrogen bond; electrostatic interaction; topological analysis; donor–acceptor systems

1. Introduction

Inter- and intramolecular hydrogen bonds (HBs) are important factors governing interactions, structures and conformations of molecules and have long been studied by spectroscopists and crystallographers.[1–5] HB interactions are, in general, weaker than ionic and covalent bonds but have a profound effect on many chemical and physical properties and determine the shapes of large molecules, such as proteins and nucleic acids.[6] The classical definition of the HB considers it as an electrostatic interaction between a positively charged H atom and an electronegative atom X having almost one lone pair (usually F, O or N).[7] Many aspects of HBs in structural chemistry and biology can be readily explained at this level, and it is certainly the relative success of these views that has made them dominate the perception of the HB for decades.[8–10] However, many unusual HBs have been found and general definitions, such as the aforementioned classical definition, became obsolete after each new finding. Indeed, it was experimentally discovered that carbon atoms may act as proton donors (C—H···Y),[11] that unsaturated bonds may act as proton acceptors (X—H···π) and that even hydrogen atoms may be acceptors in the so-called dihydrogen ($H^{\delta-}\cdots H^{\delta+}$) and hydrogen–hydrogen bonds (H···H), among other unusual HBs.[12–14] Thus, even though strong HBs tend to adopt a linear arrangement, there is not a default behaviour for such interactions, challenging the scientific community to search for approaches to characterise and understand them.[12–16]

Herein, we present an alternative representation of HBs in the domain of quantum chemical topology, a subarea of quantum mechanics.[17] In particular, the quantum theory of atoms in molecules (QTAIMs) and the electron localisation functions (ELFs) [18–20] were applied, which are widely used and considered highly reliable theoretical methods for the characterisation of HBs and other long-range interactions, even in difficult and ambiguous situations.[18–31]

Both the QTAIM and ELF methods use the electron density (ρ) as the source of information. They are routinely used to characterise HBs, especially QTAIMs. In this context, some useful criteria to characterise the formation of HBs, based on the QTAIM parameters, were developed by Popelier [30,31], which may be summarised as follows: (1) topological consistency: formation of a bond critical point (BCP) for the HB; (2) the HB BCP electron density (ρ_{HBCP}) and its Laplacian ($\nabla^2\rho_{HBCP}$) should lie in the range of 0.002–0.040 a.u. and 0.024–0.139 a.u., respectively; (3) there must be a mutual penetration between the hydrogen and acceptor atoms. This interpenetration is quantified by $\Delta r_H = r_H^0 - r_H$ and by $\Delta r_B = r_B^0 - r_H$, where r_H^0 and r_B^0 are the non-bonding radii of hydrogen and acceptor atoms (we approximate the r_H^0 and r_B^0 measurement by the shortest distance of the corresponding nucleus to the 0.001 a.u. surface contour in a conformer not involved in the HB) and r_H and r_B are the bonding radii of the hydrogen and acceptor atoms (measured by the

*Corresponding author. Email: rittner@iqm.unicamp.br

distance of each atom to the HB BCP), respectively; (4) the hydrogen atom loses electrons, i.e. its atomic charge [q(H)] decreases; (5) the hydrogen atom is destabilised in the complexation, which is measured by the variation of [ΔE(H)]; (6) the magnitude of the first dipole moment [$M_1(\Omega)$] in hydrogen diminishes and (7) the hydrogen volume [V(H)] decreases with complexation.

Although the ELF method for topological analysis is based on the same concept of gradient paths as the QTAIM, the fundamentals of these two theories are quite different. The ELF is a function that measures the Pauli repulsion on the kinetic energy density and has a value close to zero if there is a high probability of finding close same spin electrons, which implies electron delocalisation, and close to unity if there is low probability of finding close same spin electrons, which implies electron localisation.[32,33] Concerning HB, the ELF method is less popular than QTAIM, but it has been shown to be a powerful tool to characterise HB through the so-called core-valence bifurcation index (CVBI) and may be used complementarily to the QTAIM [20,34,35] analysis. Considering a general X—H···Y HB, the CVBI may be defined as $\eta(r_{CV}) - \eta(r_{XHY})$,[36] where $\eta(r_{CV})$ is the ELF value at the critical point between the core basin of the proton donor X atom [C(X)] and the disynaptic valence basin of the X—H bond [V(X, H)], and $\eta(r_{XHY})$ is the value at the critical point between the V(X, H) and the core basin of the proton acceptor Y atom [C(Y)]. For relatively strong and very strong HBs, the CVBI has negative values, while for relatively medium and weak HBs, CVBI values are positive. It is important to note that it has been proven that the localisation of critical points found by the QTAIM and ELF methods is coincident.[34–36] Moreover, HBs are interactions without borders and may behave either as a weak electrostatic van der Waals interaction or even as a strong bond with covalent character.[20] The QTAIM, through the total electron energy at the HB BCP (H_{HBCP}) value,[37] has recently been used to obtain insights into the origins of this important intermolecular interaction, particularly those related to its electrostatic/covalent character.

In the present report, the electron properties of linear and angular HX···HX and CH_3X···HX dimers (X = Br, Cl and F) have been characterised by using QTAIM and ELF methods. Special emphasis has been given to the different interactions present in the complexes.

2. Computational methods

In this work, all calculations were carried out with the Gaussian 09 package,[38] while AIMALL [39] and TopMod [40] packages were used in the QTAIM and

Table 1. HB energies (E_{HB}) in kcal mol^{-1} and bond lengths (in Å) for the linear HX···HX and CH_3X···HX dimer equilibrium geometries.

	HX···HX dimmers			
	r(HX···HX)	r[H–X(1)][a]	r[H–X(2)]	E_{HB}
HBr(1)···HBr(2)	3.162	1.407	1.407	−0.18
HBr···HCl	3.384	1.407	1.275	−0.05
HBr···HF	7.558	1.407	0.922	–
HCl···HBr	2.944	1.275	1.407	−0.41
HCl(1)···HCl(2)	2.994	1.275	1.275	−0.32
HCl···HF	3.682	1.275	0.922	−0.13
HF···HBr	2.205	0.923	1.409	−1.99
HF···HCl	2.136	0.923	1.277	−2.29
HF(1)···HF(2)	1.947	0.923	0.925	−3.30
	CH_3X···HX dimmers			
	r(CH_3X···HX)	r(CH_3–X)[b]	r(H–X)	E_{HB}
CH_3Br···HBr	2.880	1.927	1.408	−0.84
CH_3Br···HCl	2.919	1.927	1.276	−0.72
CH_3Br···HF	3.124	1.927	0.922	−0.45
CH_3Cl···HBr	2.699	1.783	1.408	−1.13
CH_3Cl···HCl	2.700	1.783	1.276	−1.08
CH_3Cl···HF	2.714	1.784	0.923	−0.98
CH_3F···HBr	2.103	1.395	1.410	−2.65
CH_3F···HCl	2.041	1.396	1.279	−3.03
CH_3F···HF	1.865	1.398	0.927	−4.30

[a] r(H—X) monomer distances = 1.407, 1.275 and 0.922 for X = Br, Cl and F, respectively.
[b] r(CH_3—X) monomer distances = 1.925, 1.780 and 1.388 for X = Br, Cl and F, respectively.

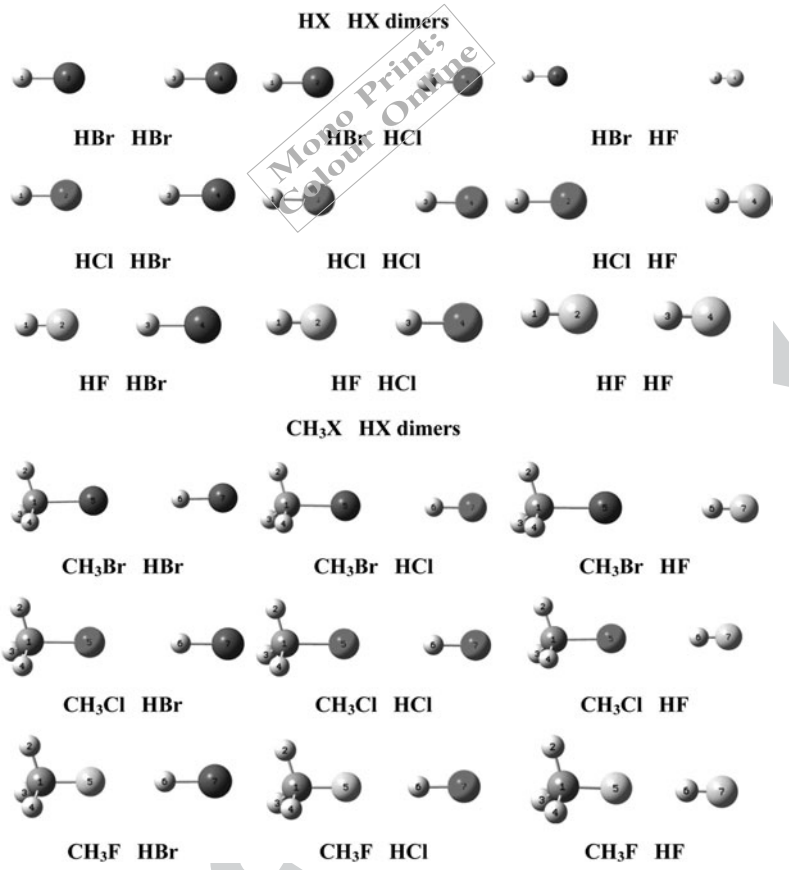

Figure 1. Graphical representations of the HX···HX and CH_3X···HX linear dimer arrangement equilibrium geometries.

ELF analyses, respectively. The structures of monomers and dimers were fully optimised at the MP2/aug-cc-pVTZ level with the counterpoise basis set superposition error correction [41] included in the optimisation step. The energy minima were identified by building potential energy surfaces (PESs), obtained through scanning the linear and angular dimer distances in steps of 0.03 Å from the equilibrium geometry.

The QTAIM and ELF topological analyses were applied over the wave functions obtained from the MP2/aug-cc-pVTZ equilibrium geometries ('density = current' keyword was used in the Gaussian09 program). The

Table 2. Electronic density, electronic density Laplacian, total electron density energy at the HB BCP (ρ, $\nabla^2\rho$ and H_c, respectively) and integrated atomic properties of the H3 atom in a.u. and atomic distances in Å for the linear HX···HX dimer arrangements.

	ρ	$\nabla^2\rho$	q(H3)	E(H3)	M_1(H3)	V(H3)	r_{H3}	Δr_{H3}[a]	r_{X2}	Δr^a_{X2}	H_c
H—Br	–	–	+0.104	−0.5421	0.083	46.374	–	–	–	–	–
H—Cl	–	–	+0.298	−0.4797	0.136	36.122	–	–	–	–	–
H—F	–	–	+0.753	−0.2532	0.118	13.972	–	–	–	–	–
HBr···HBr	0.003	+0.011	+0.073	−0.5397	0.059	49.571	1.21	0.08	1.949	0.09	+0.0007
HBr···HCl	0.002	+0.007	+0.297	−0.4671	0.130	37.759	1.30	−0.01	2.082	−0.04	+0.0005
HBr···HF	–	–	+0.782	−0.2273	0.103	12.008	–	–	–	–	–
HCl···HBr	0.004	+0.015	+0.079	−0.5376	0.055	48.647	1.15	0.09	1.795	0.14	+0.0010
HCl···HCl	0.003	+0.013	+0.300	−0.4660	0.125	37.501	1.16	0.08	1.836	0.09	+0.0008
HCl···HF	0.0004	+0.002	+0.782	−0.2273	0.103	12.280	1.41	−0.17	2.269	−0.34	+0.0001
HF···HBr	0.009	+0.048	+0.128	−0.5203	0.036	41.776	0.89	0.26	1.311	0.33	+0.0025
HF···HCl	0.010	+0.054	+0.343	−0.4503	0.101	30.452	0.85	0.30	1.290	0.35	+0.0026
HF···HF	0.014	+0.076	+0.799	−0.2174	0.085	8.715	0.71	0.44	1.236	0.40	+0.0028

Note: Atom numbering in Figure 1.

[a] r^0_{H3} and r^0_X were calculated from H3 and X2 atom minimum distances to 0.001 a.u. contour surface in each corresponding monomer (HF, HCl or HBr), obtaining r^0_{X2} = 1.29, 1.24 and 1.15 Å, for HBr, HCl and HF, respectively, and r^0_{Br2} = 2.04 Å, r^0_{Cl2} = 1.93 Å and r^0_{F2} = 1.64 Å.

Table 3. Electronic density, electronic density Laplacian and total electron density energy at the HB BCP (ρ, $\nabla^2\rho$ and H_c, respectively) and integrated atomic properties of the H6 atom in a.u. and atomic distances in Å for the linear HX···HX dimer arrangements.

	ρ	$\nabla^2\rho$	q(H7)	E(H7)	M_1(H6)	V(H6)	r_{H6}	Δr_{H6}[a]	r_{X5}	Δr_{X5}[a]	H_c
H—Br	–	–	+0.104	−0.5421	0.083	46.374	–	–	–	–	–
H—Cl	–	–	+0.298	−0.4797	0.136	36.122	–	–	–	–	–
H—F	–	–	+0.753	−0.2532	0.118	13.972	–	–	–	–	–
$CH_3Br\cdots HBr$	0.010	+0.032	+0.107	−0.5426	0.068	44.979	0.95	0.34	1.70	0.34	0.0010
$CH_3Br\cdots HCl$	0.005	+0.018	+0.303	−0.4643	0.124	36.847	1.06	0.18	1.85	0.19	0.0010
$CH_3Br\cdots HF$	0.003	+0.010	+0.750	−0.2533	0.118	16.328	1.10	0.05	2.02	0.02	0.0006
$CH_3Cl\cdots HBr$	0.006	+0.026	+0.093	−0.5322	0.049	46.268	1.02	0.27	1.68	0.25	0.0014
$CH_3Cl\cdots HCl$	0.006	+0.024	+0.302	−0.4777	0.125	36.636	1.00	0.24	1.70	0.23	0.0012
$CH_3Cl\cdots HF$	0.005	+0.021	+0.751	−0.2525	0.115	15.108	0.96	0.19	1.75	0.18	0.0012
$CH_3F\cdots HBr$	0.013	+0.061	+0.154	−0.5253	0.047	39.901	0.84	0.45	1.27	0.37	0.0025
$CH_3F\cdots HCl$	0.014	+0.068	+0.339	−0.4641	0.101	30.024	0.79	0.45	1.25	0.39	0.0025
$CH_3F\cdots HF$	0.018	+0.091	+0.802	−0.2137	0.081	7.735	0.66	0.49	1.20	0.44	0.0023

Note: Atom numbering in Figure 1.
[a] r^0_{H6} and r^0_X were calculated from H6 and X5 atom minimum distances to 0.001 a.u. contour surface in each corresponding monomer (HF, HCl or HBr), obtaining r^0_{X6} = 1.29, 1.24 and 1.15 Å, for HBr, HCl and HF, respectively, and r^0_{Br5} = 2.04 Å, r^0_{Cl5} = 1.93 Å and r^0_{F5} = 1.64 Å.

QTAIM local BCP has been already defined. The QTAIM zero flux surfaces construction qualities were obtained by the integrated Laplacian of ρ values over Ω [L(Ω)], which were always lower than 10^{-3} a.u. The topological analysis of the ELF gradient field, $\nabla\eta(r)$, provides a mathematical model permitting the partitioning of the molecular position space into basins of attractors, which present, in principle, a one-to-one correspondence with local chemical objects such as bonds and lone pairs.[42,43] The ELF calculations were computed over a grid spacing of 0.1 a.u. for each compound, and the isosurfaces were obtained for an ELF value of 0.8 a.u. Several applications of ELFs to various molecules, atomic clusters, molecular clusters, HB interactions and even to solid systems indicate that this technique yields meaningful, easily understandable and visually directive patterns of the interactions between vicinal atoms.[44–47] A complete description of the ELF concepts can be found elsewhere.[21,32,48]

Table 4. ELF values at the critical point between C(X) and V (X, H) [$\eta(r_{DHX})$] and at the critical point between V(X, H) and V (X) [$\eta(r_{CV})$] and the core valence bond index [CVBI = $\eta(r_{CV})$ – $\eta(r_{DHX})$] for the HX···HX and $CH_3X\cdots HX$ linear dimer arrangements in a.u.

	HX···HX dimmers		
	$\eta(r_{DHX})$	$\eta(r_{CV})$	CVBI
HBr···HBr	0.003	0.132	0.129
HBr···HCl	0.001	0.078	0.077
HBr···HF	0.000	0.084	–
HCl···HBr	0.005	0.132	0.127
HCl···HCl	0.003	0.078	0.075
HCl···HF	0.000	0.084	0.084
HF···HBr	0.013	0.134	0.121
HF···HCl	0.014	0.078	0.064
HF···HF	0.019	0.086	0.066
	$CH_3X\cdots HX$ dimers		
	$\eta(r_{DHX})$	$\eta(r_{CV})$	CVBI
$CH_3Br\cdots HBr$	0.024	0.165	0.141
$CH_3Br\cdots HCl$	0.007	0.163	0.157
$CH_3Br\cdots HF$	0.002	0.173	0.171
$CH_3Cl\cdots HBr$	0.011	0.075	0.064
$CH_3Cl\cdots HCl$	0.011	0.077	0.066
$CH_3Cl\cdots HF$	0.007	0.076	0.069
$CH_3F\cdots HBr$	0.021	0.107	0.086
$CH_3F\cdots HCl$	0.024	0.117	0.093
$CH_3F\cdots HF$	0.028	0.093	0.065

3. Results and discussion

Initially, a linear arrangement for the dimeric compounds HX···HX and $CH_3X\cdots HX$ (X = F, Cl and Br) was used to evaluate the HB energies. It is well known that this geometry is not preferential, but it may be formed in cases where geometric restrictions take place and, to the best of our knowledge, it has not been previously studied in the literature for these dimers. To estimate the HB energy (E_{HB}) in the linear arrangement of HX···HX and $CH_3X\cdots HX$ (X = F, Cl and Br) dimers, their *ab initio* MP2/aug-cc-pVTZ energies and equilibrium geometries were obtained (Table 1 and Figure 1). A detailed analysis of the E_{HB} values reported in Table 1 shows that for both HX···HX and $CH_3X\cdots HX$ dimers, when Br and Cl atoms act as proton acceptors, they form stronger HBs with HBr and HCl than with HF, i.e. the X···H—Br (X = Br or Cl) interactions are stronger than X···H—Cl, which in turn are stronger than X···H—F. Indeed, in the HBr···HF case, the corresponding dimer is not formed. However, F atoms form the strongest HB in the linear model when acting as proton acceptors. For $CH_3X\cdots HX$, it is important to note that HB acceptor F atoms, when acting as proton acceptors, form the strongest HB in the linear model. For

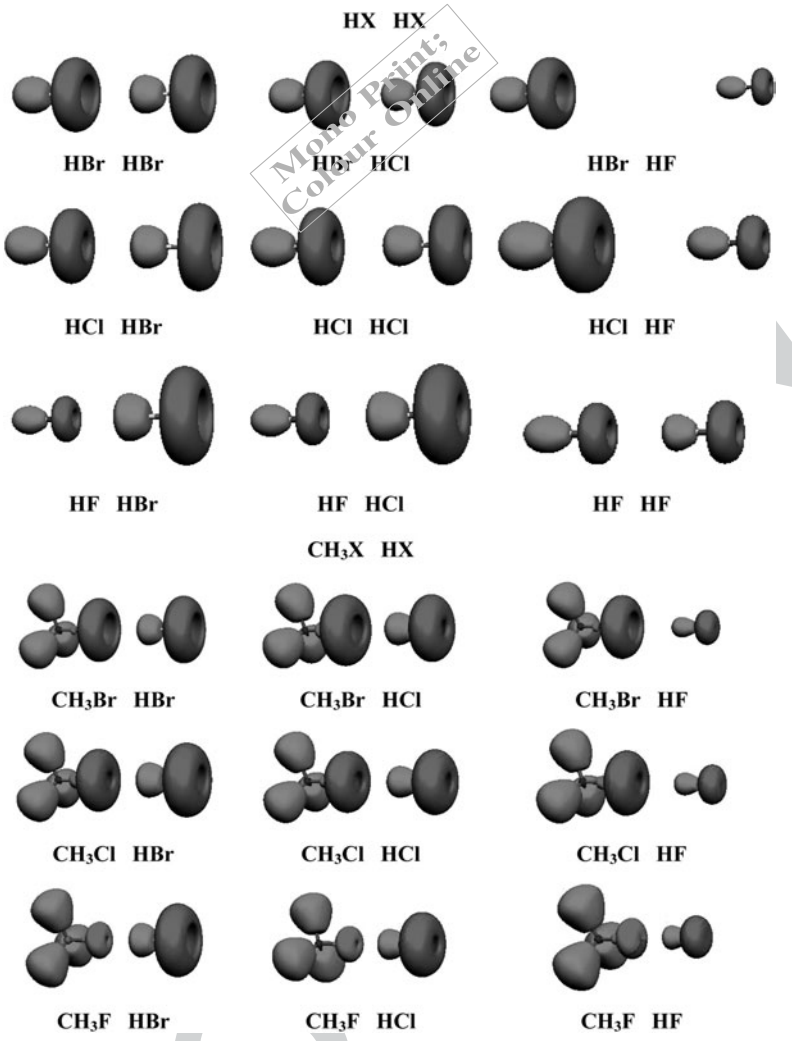

Figure 2. ELF isosurfaces for the linear arrangement of the HX···HX and CH_3···HX dimers.

CH_3X···HX, it is important to note that HB acceptor F atoms form stronger HBs because it has been shown, with several examples in the literature, that F atoms attached to C atoms (organofluorine compounds) hardly ever participate in HBs, while, on the other hand, the F atom acts as a very strong proton acceptor.[49,50] However, this is not the case in our results, which indicate that the proton acceptor CH_3F molecule forms stronger HBs than inorganic HF compound in the linear model (Table 1).

As indicated by the HB length distances and energies in Table 1 and in the PESs (Figures S1 and S2; Supporting Information), F acting as a proton acceptor should form stronger HBs in comparison with Br and Cl, but in contrast, it needs closer contact, which in some cases is less than 2 Å.

The topological analysis through the QTAIM and ELF methods was evaluated for the linear CH_3X···HX and HX···HX dimer arrangements (QTAIM molecular graphs are shown in the Supporting Information Figure S3). In this way, the QTAIM Popelier criteria [30] and Rozas et al's total energy at the BCP (H_c) parameter [37] (Tables 2 and 3) and the ELF CVBI parameter (Table 4) were obtained for all linear dimers. The local measure of the density at the BCP has often been treated as a measure of the HB strength because it correlates with HB energies. [51–53] As a general trend, a weaker HB is related to lower density in the BCP. The Popelier criteria (Tables 2 and 3) are not fulfilled by the HBr···HCl, HBr···HF (there is no stabilising interaction in this case) and HCl···HF. In fact, all QTAIM parameters indicated in Tables 2 and 3 agree with the E_{HB} values and highlight the HB force trend for these dimers. In addition, the ELF CVBI values shown in Table 4 (The ELF values along the XH···X contact line are shown in Supporting Information Figures S4 and S5) agree with the E_{HB} and QTAIM results. ELF isosurfaces (Figure 2) also show an interesting behaviour for the linear arrangement and indicate that the halogen electron pairs are distributed in a toroidal ring form, which is in a

Table 5. HB energies (E_{HB}) in kcal mol^{-1} and bond lengths (in Å) for the nonlinear HX···HX and CH_3X···HX dimer equilibrium geometries.

	HX···HX dimmers				
	r(HX···HX)	r[H—X(1)][a]	r[H—X(2)]	∠ H—X···H	E_{HB}
HBr(1)···HBr(2)	2.724	1.408	1.411	87.87	−1.86
HBr···HCl	2.674	1.408	1.280	88.96	−2.00
HBr···HF	2.505	1.409	0.927	91.01	−2.60
HCl···HBr	2.600	1.276	1.411	90.30	−1.83
HCl(1)···HCl(2)	2.538	1.276	1.279	91.11	−2.03
HCl···HF	2.346	1.277	0.927	92.65	−2.79
HF···HBr	2.161	0.924	1.410	122.09	−2.24
HF···HCl	2.083	0.924	1.279	120.04	−2.66
HF(1)···HF(2)	1.852	0.925	0.928	115.04	−4.23
	CH_3X···HX dimmers				
	r(CH_3X···HX)	r(CH_3–X)[b]	r(H—X)	∠ C—X···H	E_{HB}
CH_3Br···HBr	2.567	1.929	1.416	81.9	−3.38
CH_3Br···HCl	2.539	1.930	1.284	82.3	−3.53
CH_3Br···HF	2.402	1.931	0.930	85.4	−4.20
CH_3Cl···HBr	2.436	1.786	1.415	86.3	−3.34
CH_3Cl···HCl	2.391	1.786	1.284	86.8	−3.56
CH_3Cl···HF	2.242	1.789	0.931	90.6	−4.50
CH_3F···HBr	2.045	1.398	1.413	109.6	−3.17
CH_3F···HCl	1.972	1.399	1.283	110.3	−3.65
CH_3F···HF	1.771	1.404	0.930	113.4	−5.43

[a] r(H—X) monomer distances = 1.407, 1.275 and 0.922 for X = Br, Cl and F, respectively.
[b] r(CH_3—X) monomer distances = 1.925, 1.780 and 1.388 for X = Br, Cl and F, respectively.

perpendicular direction from the H—X/C—X bonds, as one may expect in the Linnett theory basis.[54] Such toroidal rings appear less stable for the F atom lone pairs, which have an approximately spherical distribution. Thus, this halogen lone pair shape may indicate that angular geometries should be preferential for CH_3X···HX and HX···HX dimer arrangements, but that for F acting as a proton acceptor, it should not be as important as for Cl and Br atoms.

In the next step, the angular arrangements for the CH_3X···HX and HX···HX dimers were analysed (PESs are shown in the Supporting Information, Figures S6 and S7). The geometrical parameters and E_{HB} values are shown in Table 5, and their graphical representations are depicted in Figure 3. By comparing the E_{HB} values in Tables 1 and 5, it is clear that HBs in the angular arrangements are stronger than in the linear arrangements and that, in contrast to the linear model, Br and Cl acting

Table 6. Electronic density, electronic density Laplacian and total electron density energy at the HB BCP(ρ, $\nabla^2\rho$ and H_c, respectively) and integrated atomic properties of the H3 atom in a.u. and atomic distances in Å for the nonlinear HX···HX dimers.

	ρ	$\nabla 2\rho$	q(H3)	E(H3)	M_1(H3)	V(H3)	r_{H3}	Δr_{H3}[a]	rX2	Δr_{X2}[a]	H_c
H—Br	–	–	**+0.104**	**−0.5421**	**0.083**	**46.374**	–	–	–	–	–
H—Cl	–	–	**+0.298**	**−0.4797**	**0.136**	**36.122**	–	–	–	–	–
H—F	–	–	**+0.753**	**−0.2532**	**0.118**	**13.972**	–	–	–	–	–
HBr···HBr	0.011	+0.030	+0.108	−0.5234	0.051	43.829	0.92	0.37	1.80	0.24	0.0009
HBr···HCl	0.011	+0.032	+0.322	−0.4540	0.117	32.882	0.89	0.40	1.79	0.25	0.0008
HBr···HF	0.014	+0.039	+0.781	−0.2222	0.100	10.049	0.77	0.52	1.74	0.30	0.0002
HCl···HBr	0.011	+0.035	+0.113	−0.5233	0.047	43.160	0.91	0.33	1.69	0.24	0.0013
HCl···HCl	0.012	+0.038	+0.327	−0.4533	0.113	32.164	0.87	0.37	1.67	0.26	0.0012
HCl···HF	0.016	+0.048	+0.785	−0.2209	0.096	9.420	0.74	0.50	1.61	0.32	0.0004
HF···HBr	0.012	+0.055	+0.136	−0.5169	0.034	40.456	0.85	0.30	1.31	0.33	0.0024
HF···HCl	0.014	+0.064	+0.351	−0.4465	0.098	29.330	0.80	0.35	1.29	0.35	0.0024
HF···HF	0.021	+0.095	+0.802	−0.2143	0.081	7.502	0.64	0.51	1.21	0.43	0.0015

Note: Atom numbering in Figure 3.
[a] r^0_{H3} and r^0_X were calculated from H3 and X2 atom minimum distances to 0.001 a.u. contour surface in each corresponding monomer (HF, HCl or HBr), obtaining r^0_{X2} = 1.29, 1.24 and 1.15 Å, for HBr, HCl and HF, respectively, and r^0_{Br2} = 2.04 Å, r^0_{Cl2} = 1.93 Å and r^0_{F2} = 1.64 Å.

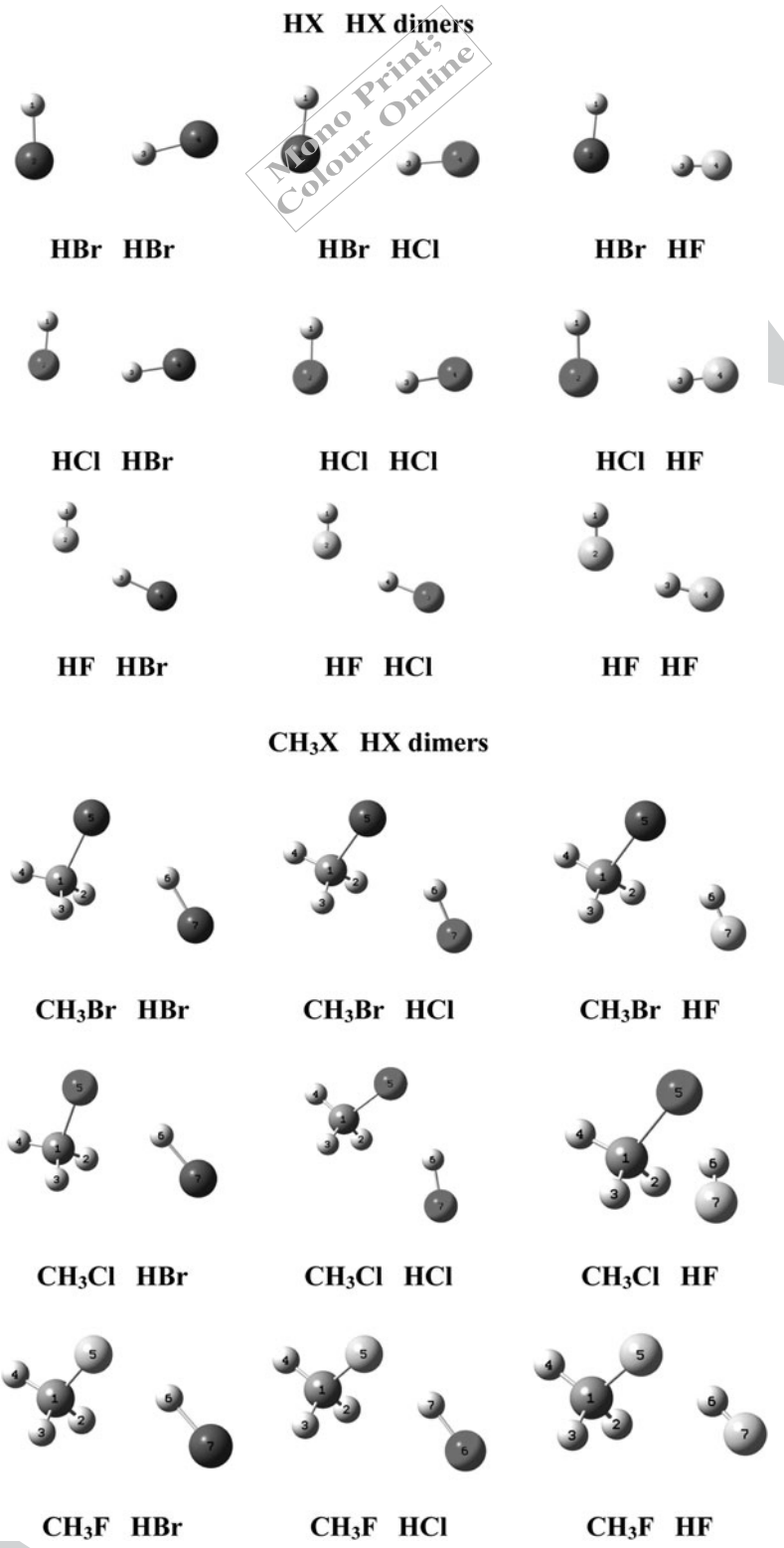

Figure 3. Graphical representations of the nonlinear arrangement HX···HX and CH_3X···HX dimer equilibrium geometries.

Table 7. Electronic density, electronic density Laplacian and total electron density energy at the HB BCP (ρ, $\nabla^2\rho$ and H_c, respectively) and integrated atomic properties of the H6 atom in a.u. and atomic distances in Å for the nonlinear $CH_3X\cdots CH_3X$ dimer arrangements.

	ρ	$\nabla^2\rho$	q(H6)	E(H6)	M_1(H6)	V(H6)	r_{H6}	Δr_{H6}[a]	r_{X5}	Δr_{X5} [a]	H_c
H—Br	–	–	**+0.104**	**−0.5421**	**0.083**	**46.374**	–	–	–	–	–
H—Cl	–	–	**+0.298**	**−0.4797**	**0.136**	**36.122**	–	–	–	–	–
H—F	–	–	**+0.753**	**−0.2532**	**0.118**	**13.972**	–	–	–	–	–
$CH_3Br\cdots HBr$	0.015	+0.040	+0.133	−0.51330	0.049	39.432	0.855	0.44	1.714	0.33	+0.0005
$CH_3Br\cdots HCl$	0.016	+0.041	+0.337	−0.4462	0.113	29.591	0.828	0.41	1.709	0.22	+0.0004
$CH_3Br\cdots HF$	0.018	+0.046	+0.783	−0.2192	0.098	9.398	0.726	0.42	1.676	−0.04	−0.0006
$CH_3Cl\cdots HBr$	0.016	+0.047	+0.139	−0.5123	0.045	38.665	0.830	0.46	1.605	0.44	+0.0009
$CH_3Cl\cdots HCl$	0.017	+0.050	+0.345	−0.4447	0.107	28.624	0.798	0.44	1.593	0.34	+0.0007
$CH_3Cl\cdots HF$	0.021	+0.057	+0.788	−0.2173	0.093	8.719	0.691	0.46	1.551	0.09	−0.0008
$CH_3F\cdots HBr$	0.017	+0.074	+0.157	−0.5094	0.033	37.355	0.780	0.51	1.266	0.77	+0.0026
$CH_3F\cdots HCl$	0.019	+0.083	+0.367	−0.43958	0.092	26.749	0.732	0.51	1.242	0.69	+0.0025
$CH_3F\cdots HF$	0.028	+0.111	+0.807	−0.2107	0.077	6.731	0.594	0.56	1.178	0.46	−0.0003

Note: Atom numbering in Figure 3.
[a] r^0_{H6} and r^0_X were calculated from H6 and X5 atom minimum distances to 0.001 a.u. contour surface in each corresponding monomer (HF, HCl or HBr), obtaining r^0_{X7} = 1.29, 1.24 and 1.15 Å, for HBr, HCl and HF, respectively, and r^0_{Br5} = 2.04 Å, r^0_{Cl5} = 1.93 Å and r^0_{F5} = 1.64 Å.

as proton acceptors form stronger HBs, according to the expected proton donor ability, i.e. X···HF > X···HCl > X···HBr. More interestingly, as we are expecting from the ELF isosurfaces (Figure 2), the HB energy values for Br and Cl atoms acting as proton acceptors increased by more than 2 kcal mol^{-1} in some cases from the linear to the angular model, while the highest increase in energy for the F atom was only 1 kcal mol^{-1} in the strongest HB $CH_3F\cdots HF$ dimer. Indeed, the nonlinear $CH_3X\cdots HX$ and $HX\cdots HX$ dimer arrangement ELF isosurfaces (Figure S8 in Supporting Information) show that the HB interactions are directed towards the halogen lone pairs toroidal ring and, consequently, indicate that HBs in angular geometries should be stronger than in the linear geometries.

Table 8. ELF values at the critical point between C(X) and V(X, H) [$\eta(r_{DHX})$] and at the critical point between V(X, H) and V(X) [$\eta(r_{CV})$] and the core valence bond index [CVBI $= \eta(r_{CV}) - \eta(r_{DHX})$] for the HX···HX and $CH_3X\cdots HX$ nonlinear dimer arrangements in a.u.

	HX···HX dimmers		
	$\eta(r_{DHX})$	$\eta(r_{CV})$	CVBI
HBr···HBr	0.037	0.139	0.102
HBr···HCl	0.038	0.078	0.040
HBr···HF	0.047	0.085	0.038
HCl···HBr	0.032	0.134	0.102
HCl···HCl	0.035	0.078	0.043
HCl···HF	0.046	0.085	0.039
HF···HBr	0.021	0.134	0.113
HF···HCl	0.025	0.079	0.054
HF···HF	0.041	0.086	0.045
	$CH_3X\cdots HX$ dimers		
	$\eta(r_{DHX})$	$\eta(r_{CV})$	CVBI
$CH_3Br\cdots HBr$	0.061	0.167	0.106
$CH_3Br\cdots HCl$	0.061	0.169	0.108
$CH_3Br\cdots HF$	0.068	0.166	0.098
$CH_3Cl\cdots HBr$	0.056	0.089	0.033
$CH_3Cl\cdots HCl$	0.059	0.087	0.038
$CH_3Cl\cdots HF$	0.069	0.095	0.026
$CH_3F\cdots HBr$	0.034	0.154	0.120
$CH_3F\cdots HCl$	0.039	0.158	0.119
$CH_3F\cdots HF$	0.058	0.133	0.075

A plethora of theoretical and experimental investigation has been carried out in order to understand the catalytic role of HB donor molecules along the course of chemical reactions, in particular the effect of the presence of Lewis acids on the hetero Diels–Alder rearrangement, [55,56] suggesting that this type of HB interactions accelerates the hetero-Diels–Alder reaction.

Furthermore, the HB nonlinear QTAIM parameters (molecular graphs are shown in Figure S9, Supporting Information), reported in Tables 6 and 7, indicate that angular HBs are stronger than HBs in the linear arrangement. In fact, unlike the linear model, even the HBr···HCl, HBr···HF and HCl···HF complexes fulfil the Popelier criteria. In addition, the negative values for the H_c parameter indicate that the organic $CH_3Br\cdots HF$, $CH_3Cl\cdots HF$ and $CH_3F\cdots HF$ dimers have a covalent character and are the strongest interactions (Table 7), which is in agreement with the E_{HB} values given in Table 5. The ELF CVBI values described in Table 8 (ELF values along the XH···X contact are shown in Figures S10 and S11, Supporting Information) are also in agreement with the E_{HB} and QTAIM parameters (see Tables 5–8). Thus, all applied methods in this work suggest that the nonlinear arrangements should form stronger HBs than the linear arrangements and that $CH_3X\cdots HX$ dimers may form stronger HBs than HX···HX complexes.

4. Conclusions

Our results, which are based on the QTAIM and ELF methods, suggest that F is a better proton acceptor than Br and Cl atoms in linear and angular geometries of $CH_3X\cdots HX$ and $HX\cdots HX$ dimers, but it needs shorter HB contacts because F atoms are less polarisable than Cl and Br atoms. Moreover, our results indicate that organic CH_3X compounds are better proton acceptors than inorganic HX compounds for the cases studied here. Furthermore, angular $CH_3X\cdots HX$ and $HX\cdots HX$ arrangements form stronger HBs than linear arrangements, which, as indicated by the ELF isosurfaces, is a consequence of the halogen lone pairs toroidal ring shape. We hope that these findings may be helpful in clarifying the interaction mode of HB-based complexes, in understanding HBs involving halogen atoms in inorganic and organic compounds, as well as in driving synthesis of ligands with improved hydrogen donor or acceptor ability towards a biological target.

Acknowledgements

The authors are grateful to FAPESP and FAPEMIG for financially supporting this research and for a scholarship (to R.A.C.), to CAPES for the scholarships (to F.A.L. and R.T.S.) and to CNPq for the fellowships (to T.C.R., M.P.F., E.F.F.C. and R.R.). J.A. also thanks Universitat Jaume I-Fundación Bancaixa (Project P1.1B2010-10), Generalitat Valenciana for Prometeo/2009/053 project, Ministerio de Ciencia e Innovación for project CTQ2009-14541-C02 and Programa de Cooperación Científica con Iberoamerica (Brazil), Ministerio de Educación (PHB2009-0065-PC).

References

[1] Zieliński W, Katrusiak A. Hydrogen bonds NH···N in compressed benzimidazole polymorphs. Cryst Growth Des. 2013;13:696–700.
[2] Ibrahim MAA. Molecular mechanical study of halogen bonding in drug discovery. J Comput Chem. 2011;32:2564–2574.
[3] Corradi E, Meile SV, Messina MT, Metrangolo P, Resnati G. Halogen bonding versus hydrogen bonding in driving self-assembly processes. Angew Chem Int Ed. 2000;39:1782–1786.
[4] de Oliveira BG. Structure, energy, vibrational spectrum, and Bader's analysis of (π···H hydrogen bonds and $H^{-\delta}\cdots H^{+\delta}$ dihydrogen bonds. Phys Chem Chem Phys. 2013;15:37–79.
[5] Freitas MP, Tormena CF, Rittner R, Abraham RJ. Conformational analysis of trans-2-halocyclohexanols and their methyl ethers: a ^{1}H NMR, theoretical and solvation approach. J Phys Org Chem. 2003;16:27–33.
[6] Rauk A. Orbital interaction theory of organic chemistry. New York, NY: Wiley; 2000.
[7] Steiner T, Saenger W. Distribution of observed C—H bond lengths in neutron crystal structures and temperature dependence of the mean values. Acta Crystallogr A. 1993;49:379–384.
[8] Smith DA. Modeling the hydrogen bond. Washington, DC: American Chemical Society Series; 1994.
[9] Steiner T. The hydrogen bond in the solid state. Angew Chem Int Ed. 2002;41:48–76.
[10] Szatylowicz H, Krygowski TM, Guerra CF, Bickelhaupt FM. Complexes of 4-substituted phenolates with HF and HCN: energy decomposition and electronic structure analyses of hydrogen bonding. J Comput Chem. 2013;34:696–705.
[11] Gilli G, Gilli P. The nature of the hydrogen bond: outline of a comprehensive hydrogen bond theory. New York, NY: Oxford University Press; 2009.
[12] Sutor DJ. The crystal and molecular structure of β-alanine. Nature. 1964;195:68. [Q2]
[13] Bakhmutov VI. Dihydrogen bonds: principles, experiments and applications. NJ: Wiley; 2008. [Q3]
[14] Heinekey DM, Lledós A, Lluch JM. Elongated dihydrogen complexes: what remains of the H—H bond? Chem Soc Rev. 2004;33:175–182.
[15] Gilli P, Gilli G. Hydrogen bond models and theories: the dual hydrogen bond model and its consequences. J Mol Struct. 2010;972:2–10.
[16] Michael M. The ionic hydrogen bond. Chem Rev. 2005;105:213–284.
[17] Hohenberg P, Kohn W. Inhomogeneous electron gas. Phys Rev B. 1964;136:B864–B871.
[18] Bader RFW. Atoms in molecules: a quantum theory. Oxford: Clarendon; 1990.
[19] Bader RFW, Nguyendang TT, Tal YA. Topological theory of molecular-structure. Rep Prog Phys. 1981;44:893–948.
[20] Grabowski SJ. What is the covalency of hydrogen bonding? Chem Rev. 2011;111:2597–2625.
[21] Silvi B, Savin A. Classification of chemical-bonds based on topological analysis of electron localization functions. Nature. 1994;371:683–686.
[22] Grabowski SJ. Hydrogen bonding – new insights. Dordrecht: Springer; 2006.
[23] Graton J, Wang Z, Brossard A-M, Monteiro DG, Le Questel J-Y, Linclau B. An unexpected and significantly lower hydrogen-bond-donating capacity of fluorohydrins compared to nonfluorinated alcohols. Angew Chem Int Ed. 2012;51:6176–6180.
[24] Cormanich RA, Ducati LC, Rittner R. Are hydrogen bonds responsible for glycine conformational preferences? Chem Phys. 2011;387:85–91.
[25] Cormanich RA, Moreira MA, Freitas MP, Ramalho TC, Anconi CPA, Rittner R, Contreras RH, Tormena CF. $^{1h}J_{FH}$ coupling in 2-fluorophenol revisited: is intramolecular hydrogen bond responsible for this long-range coupling? Magn Reson Chem. 2011;49:763–767.
[26] Cormanich RA, Freitas MP, Tormena CF, Rittner R. The F···HO intramolecular hydrogen bond forming five-membered rings hardly appear in monocyclic organofluorine compounds. RSC Adv. 2012;2:4169–4174.
[27] Fonseca TAO, Freitas MP, Cormanich RA, Ramalho TC, Tormena CF, Rittner R. Computational evidence for intramolecular hydrogen bonding and nonbonding X center dot center dot center dot O interactions in 2′-haloflavonols. Beilstein J Org Chem. 2012;8:112–117.
[28] Silla JM, Cormanich RA, Rittner R, Freitas MP. Conformational analysis and intramolecular interactions in aminofluorobenzoic acids. J Phys Chem A. 2013;117:1659–1664.
[29] Mo Y. Can QTAIM topological parameters be a measure of hydrogen bonding strength? J Phys Chem A. 2012;116:5240–5246.
[30] Koch U, Popelier PLA. Characterization of C—H—O hydrogen-bonds on the basis of the charge-density. J Phys Chem A. 1995;99:9747–9754.
[31] Popelier PLA. Characterization of a dihydrogen bond on the basis of the electron density. J Phys Chem A. 1998;102:1873–1880.
[32] Savin A, Becke AD, Flad J, Nesper R, Preuss H, Vonschnering HG. A new look at electron localization. Angew Chem Int Ed. 1991;30:409–412.
[33] Savin A, Silvi B, Colonna F. Topological analysis of the electron localization function applied to delocalized bonds. Can J Chem. 1996;74:1088–1096.
[34] Navarrete-Lopez AM, Garza J, Vargas R. Relationship between the critical points found by the electron localization function and atoms in molecules approaches in adducts with hydrogen bonds. J Phys Chem A. 2007;111:11147–11152.
[35] Fuster F, Grabowski SJ. Intramolecular hydrogen bonds: the QTAIM and ELF characteristics. J Phys Chem A. 2011;115:10078–10086.

[36] Fuster F, Silvi B. Does the topological approach characterize the hydrogen bond? Theor Chem Acc. 2000;104:13–21.
[37] Rozas I, Alkorta I, Elguero J. Behavior of ylides containing N, O, and C atoms as hydrogen bond acceptors. J Am Chem Soc. 2000;122:11154–11161.
[38] Frisch MJ, Trucks GW, Schlegel HB, Scuseria GE, Robb MA, Cheeseman JR, Scalmani G, Barone V, Mennucci B, Petersson GA, Nakatsuji H, Caricato M, Li X, Hratchian HP, Izmaylov AF, Bloino J, Zheng G, Sonnenberg JL, Hada M, Ehara M, Toyota K, Fukuda R, Hasegawa J, Ishida M, Nakajima T, Honda Y, Kitao O, Nakai H, Vreven T, Montgomery JA Jr, Peralta JE, Ogliaro F, Bearpark M, Heyd JJ, Brothers E, Kudin KN, Staroverov VN, Kobayashi R, Normand J, Raghavachari K, Rendell A, Burant JC, Iyengar SS, Tomasi J, Cossi M, Rega N, Millam NJ, Klene M, Knox JE, Cross JB, Bakken V, Adamo C, Jaramillo J, Gomperts R, Stratmann RE, Yazyev O, Austin AJ, Cammi R, Pomelli C, Ochterski JW, Martin RL, Morokuma K, Zakrzewski VG, Voth GA, Salvador P, Dannenberg JJ, Dapprich S, Daniels AD, Farkas Ö, Foresman JB, Ortiz JV, Cioslowski J, Fox DJ. Gaussian 09, revision B.01. Wallingford, CT: Gaussian, Inc.; 2009.
[39] Todd AK, AIMAll version 13.01.27 (aim.tkgristmill.com) 2013.
[40] Noury S, Krokidis X, Fuster F, Silvi B. ToPMoD, Laboratoire de Chemie Théorique, Université Pierre et Marie Curie: París, 1999. Available from: http://www.lct.jussieu.fr/pagesperso/silvi/topmod_english.html
[41] Simon S, Duran M, Dannenberg JJ. How does basis set superposition error change the potential surfaces for hydrogen-bonded dimers? J Chem Phys. 1996;105:11024–11031.
[42] Polo V, Andres J, Castillo R, Berski S, Silvi B. Understanding the molecular mechanism of the 1,3-dipolar cycloaddition between fulminic acid and acetylene in terms of the electron localization function and catastrophe theory. Chem Eur J. 2004;10:5165–5172.
[43] Gonzalez-Navarrete P, Domingo LR, Andres J, Berski S, Silvi B. Electronic fluxes during Diels–Alder reactions involving 1,2-benzoquinones: mechanistic insights from the analysis of electron localization function and catastrophe theory. J Comput Chem. 2012;33:2400–2411.
[44] Sambrano JR, Garcia L, Andrés J, Berski S, Beltrán A. A theoretical study on the gas phase reactions of the anions NbO_3^-, NbO_5^-, and $NbO_2(OH)_2^-$ with H_2O and O_2. J Phys Chem A. 2004;108:10850–10860.
[45] Trout BL, Parrinello M. Analysis of the dissociation of H_2O in water using first-principles molecular dynamics. J Phys Chem B. 1999;103:7340–7345.
[46] Gonzalez-Navarrete P, Andrés J, Berski S. How a quantum chemical topology analysis enables prediction of electron density transfers in chemical reactions. The degenerated cope rearrangement of semibullvalene. J Phys Chem Lett. 2012;3:2500–2505.
[47] Gillet N, Chaudret R, Contreras-García J, Yang W, Silvi B, Piquemal J-P. Coupling quantum interpretative techniques: another look at chemical mechanisms in organic reactions. J Chem Theory Comput. 2012;8:3993–3997.
[48] Savin A, Nesper R, Wengert S, Fässler TF. ELF: the electron localization function. Angew Chem Int Ed. 1997;36:1808–1832.
[49] Dunitz JD, Taylor R. Organic fluorine hardly ever accepts hydrogen bonds. Chem Eur J. 1997;3:89–98.
[50] Carosati E, Sciabola S, Cruciani G. Hydrogen bonding interactions of covalenty bonded fluorine atoms: from crystallographic data to a new angular function in the GRID force field. J Med Chem. 2004;47:5114–5125.
[51] Grabowski SJ. *Ab initio* calculations on conventional and unconventional hydrogen bonds – study of the hydrogen bond strength. J Phys Chem A. 2001;105:10739–10746.
[52] Grabowski SJ. A new measure of hydrogen bonding strength – *ab initio* and atoms in molecules studies. Chem Phys Lett. 2001;338:361–366.
[53] Espinosa E, Molins E, Lecomte C. Hydrogen bond strengths by topological analyses of experimentally observed electron densities. Chem Phys Lett. 1998;285:170–173.
[54] Linnett JW. The electronic structure of molecules: a new approach. 1994.
[55] Polo V, Domingo LR, Andrés J. Toward an understanding of the catalytic role of hydrogen-bond donor solvents in the hetero-Diels–Alder reaction between acetone and butadiene derivative. J Phys Chem A. 2005;109:10438–10444.
[56] Huang Y, Rawal VH. Hydrogen-bond-promoted hetero-Diels–Alder reactions of unactivated ketones. J Am Chem Soc. 2002;124:9662–9663.

[Q4] [Q5]